Contents lists available at ScienceDirect

Arabian Journal of Chemistry

journal homepage: www.ksu.edu.sa

Effect of interlayer anions on the catalytic activity of Mg-Al layered double hydroxides for furfural and acetone aldol condensation reaction

Said Arhzaf [a], Jamal Houssaini [a], Mohammed Naciri Bennani [a], Marwa Alaqarbeh [b,*], Mohammed Bouachrine [c,d]

[a] Laboratory of Chemistry and Biology Applied to the Environment, CNRST-URL N°13, Research Team "Materials and Applied Catalysis," Chemistry Department, Moulay Ismail University, BP. 11201 Zitoune, Meknes 50000, Morocco
[b] Basic Science Department, Prince Al Hussein bin Abdullah II Academy for Civil Protection, Al-Balqa Applied University, Al-Salt 19117, Jordan
[c] Molecular Chemistry and Natural Substances Laboratory, Faculty of Science, Moulay Ismail University of Meknes 50000, Morocco
[d] Higher School of Technology (EST), University of Sultan Moulay Slimane, PB 170, Khenifra 54000 Morocco

ARTICLE INFO

Keywords:
Mg-Al Hydrotalcite
Mixed metal oxides
Aldol condensation
Furfural
Acetone

ABSTRACT

The aldol condensation reaction between furfural (F) and acetone (A), which typically produces 4-(2-Furyl)-3-buten-2-one (FA), is a critical reaction due to the application of the final product as a flavoring agent in various food items. Traditionally, this reaction is catalyzed by liquid-based catalysts. However, homogeneous liquid-base catalysis often leads to environmental damage. Solid-base catalysis is highly desirable to address the environmental issue due to liquid-base catalysis as it reduces the need for excessive solvents and reagents, thus preserving the environment. In this study, a series of Mg-Al hydrotalcites (HT) intercalated with nitrate ion (HT-NO_3), carbonate ion (HT-CO_3), or acetate ion (HT-CH_3COO) were prepared using three different coprecipitation procedures. Upon calcination at 450 °C, the solids were transformed into mixed metal oxides. Among the calcined hydrotalcites, the catalysts with acetate anion (cHT-CH_3COO) or carbonate anion (cHT-CO_3) exhibited the highest basicity and thus showed superior catalytic activity for the aldol condensation reaction. Optimal conversion and selectivity were achieved at 90 °C for 2 h using the most basic catalysts (cHT-CO_3 and cHT-CH_3COO). These catalysts yielded over 98 % conversion with FA selectivity of 76 % for cHT-CO_3 and 65 % for cHT-CH_3COO, respectively. Notably, the catalyst cHT-CH_3COO exhibited higher selectivity towards F2A (32 %) than the cHT-CO_3 catalyst (18 %). The effect of interlayer anions on the structural properties of the Mg-Al hydrotalcites was analyzed using X-ray diffraction. Fourier-transform infrared spectroscopy (FT-IR) was employed to investigate the interactions corresponding to different types of anions. The specific surface area and pore volume of the calcined Mg-Al hydrotalcites were determined using nitrogen adsorption (BET), while their total basicity was evaluated through acid-base titration. The reaction kinetics were monitored using gas chromatography.

1. Introduction

In green chemistry, several important industrial reactions, such as condensation, alkylation, and addition, are catalyzed by homogeneous bases. However, using liquid bases (e.g., NaOH, KOH, metal alkoxides) as catalysts in conjunction with solvents has a significant drawback. It generates substantial amounts of saline effluents on an industrial scale, which can harm the environment and necessitate costly subsequent treatment (Sudheesh et al., 2011). Research has recently investigated the potential of replacing liquid bases with basic solids, specifically layered double hydroxides (LDHs), to address environmental concerns. This substitution has several advantages, including reduced corrosion, improved regeneration, and enhanced recovery (Houssaini et al., 2023b). Many attempts have been made to replace typical liquid bases with basic solid catalysts, offering various benefits, including environmental, economic, and technical advantages (Houssaini et al., 2023a). LDHs are also valuable for the aldol condensation of furfural and acetone and can be used without solvents (West et al., 2008; Xing et al., 2010).

Peer review under responsibility of King Saud University.
* Corresponding author.
E-mail address: marwah.aqarbeh@emp.pha.edu.jo (M. Alaqarbeh).

https://doi.org/10.1016/j.arabjc.2023.105412
Received 30 August 2023; Accepted 30 October 2023
Available online 2 November 2023

Additionally, LDHs are highly regarded for their exceptional chemical and physical properties, as well as their ease of fabrication and cost-effectiveness. As a result, LDHs are widely used for various applications, including catalysis, batteries, cosmetics, adsorption, and sensors. (Abd El-Monaem et al., 2023; Eltaweil et al., 2023).

The aldol condensation between furfural (F) and acetone (A) generates two products, which are 4-(2-furyl)-3-buten-2-one (FA) and 1,5-difuran-2-yl-enta-1,4-dien-3-one (F2A). Furfural is produced globally from agro-food coproducts (corn cobs, wheat straw, sugar cane bagasse, etc.) through an aldol condensation reaction associated with catalytic hydrodeoxygenation, which develops potential chemical industry applications in petrochemistry and biofuel production (Serhan et al., 2019). Also, several food manufacturers use the FA as a flavoring agent for beverages, candies, gelatins, and other flavors, etc. Thus, solid catalysts based on hydrotalcite-like compounds performed the aldol condensation of furfural and acetone production by green chemical method without solvent (Parejas et al., 2019).

Hydrotalcite-like compounds belong to a class of anionic clay minerals known as layered double hydroxides (LDHs). The hydrotalcite structure resembles that of brucite Mg $(OH)_2$, in which part of the Mg^{2+} cations, coordinated octahedrally by hydroxyl ions, are replaced by Al^{3+} ions, forming positively charged layers. The general chemical formula of hydrotalcite is $[M^{2+}_{1-x}\ M^{3+}_{x}\ (OH)_2]^{x+}\ [X^{n-}_{x/n}.yH_2O]^{x-}$, where the divalent metal ion M^{2+} may include (Mg^{2+}, Zn^{2+}, Ni^{2+}…) and the trivalent metal ion M^{3+} (Al^{3+}, Fe^{3+}, Ga^{3+}…). The compensating anions X^{n-} are (CO_3^{2-}, NO_3^-, organic anions, etc.), and × is equal to the ratio of $M^{3+}/(M^{3+}+M^{2+})$ with a value varying in the range of $0.2 < x \leq 0.33$. LDHs used to a substitution of M^{2+} by M^{3+} of relatively similar sizes ($rM^{2+} - rM^{3+}$) < 0.18 Å leads to a net positive charge layer, compensated by anions in the interlayer space (Cavani et al., 1991; Miyata, 1980; Trave et al., 2002). The catalytic properties of the mixed oxides derived from hydrotalcite-like compounds are fascinating. The nature and ratio of cations present in brucite layers, the anions nature in the interlayer of the hydrotalcite precursor, and the thermal decomposition temperature notably influence the density of the basic sites (Xu et al., 1998). However, the research did not pay much attention to the influence of interlayer anions in hydrotalcite precursors on the catalytic activity of hydrotalcite-derived mixed oxides, particularly concerning aldol condensations (Tichit et al., 2003).

The advantages of layered double hydroxide-related catalysts include their low synthesis cost and high thermal stability (Abdelrahman et al., 2023; Bendary and Abdelrahman, 2022). The heterogeneously catalyzed aldol condensation of furfural and acetone using Mg-Al and rehydrated mixed oxides has received significant research attention (Arhzaf et al., 2021; Hora et al., 2015, 2014; Kikhtyanin et al., 2017, 2015; Parejas et al., 2019). Various factors have been studied to modify the physicochemical, acid-basic, and catalytic properties of the obtained oxides, including the modification of bivalent Mg and trivalent Al in the hydrotalcite-like matrix, the ratio of bivalent to trivalent ions, the synthesis method (co-precipitation, sol–gel, urea method, or hydrothermal), and the temperature of calcination of the parent hydrotalcite-like precursors (Arhzaf et al., 2020a; Debecker et al., 2009). Our long-term interest in developing basic catalysts derived from hydrotalcite-based materials, such as Mg-Al mixed oxide (Didier Tichit et al., 1998; Tichit, 1998), continues with this work. In this case, we maintain the same Mg-Al hydrotalcite-like matrix but introduce different anions in the interlayer space, specifically acetate anions. We have successfully tested mixed oxides with intercalated acetate anions as basic catalysts for the aldol condensation between furfural and acetone.

The objective of this study is to synthesize hydrotalcite HT-X with 3 M ratios of Mg/Al using the co-precipitation method and investigate the impact of intercalating different anions in the interlayer space of hydrotalcites on their physicochemical properties. Furthermore, the study aims to examine the influence of these intercalated anions on the catalytic activity and selectivity in the aldol condensation reaction between furfural and acetone using the mixed oxides obtained after heat treatment. In contrast to previous studies, this research focuses solely on mixed oxides derived from hydrotalcites that employ carbonate anions as charge compensators. Additionally, special attention is given to the effect of acetates as organic anions, as they may contribute to an enhanced selectivity in the aldol condensation reaction compared to the commonly studied carbonate anions.

2. Experimental

2.1. Materials

Magnesium nitrate ($Mg(NO_3)_2{\cdot}6H_2O$; 99 %), aluminium nitrate ($Al(NO_3)_3{\cdot}9H_2O$; 99 %), sodium carbonate (Na_2CO_3; 99.9 %), sodium hydroxide (NaOH; 99.8 %), sodium acetate ($NaCH_3CO_2$; 99.9 %), ammonia solution (NH_4OH; 25 %), Acetone (C_3H_6O; 99.8 %) and (Furfural $C_5H_4O_2$; 99.8 %) were purchased from Loba Chemie (India). ($Mg(CH_3CO_2)_2{\cdot}4H_2O$; 99.8 %), ($Al(CH_3CO_2)_2$. OH; 99.8 %), (Decane; $C_{10}H_{22}$; 99.9 %), and (FA: $C_8H_8O_2$; 99.8 %) were purchased from Sigma-Aldrich. All the reagents were of an analytical grade and were employed directly. The reaction is conducted in an autoclave reactor with a volume of 100 mL and a temperature sensor.

2.2. Catalyst preparation

2.2.1. Preparation of MgAl-X LDHs

The MgAl-CO_3 LDH was prepared by the co-precipitation method at constant pH. Two aqueous solutions (250 mL), the first one containing 0.15 mol of ($Mg(NO_3)_2{\cdot}6H_2O$) and 0.05 mol of ($Al(NO_3)_3{\cdot}9H_2O$) for a composition Mg/Al = 3 and the second one containing 0.4 mol of NaOH and 0.025 mol of Na_2CO_3, were mixed at 50 °C under vigorous stirring, maintaining the pH close to 10. The mixture was refluxed at 65 °C at the end of the addition for 18 h. The precipitate was formed and washed several times until the solution was free of nitrate ions, then dried at 80 °C. This sample is referred to as HT-CO_3.

The MgAl-NO_3- LDH was prepared, keeping the same arrangement and the exact proportions of the metal salts; the NaOH/ Na_2CO_3 precipitating agent was replaced by NH_4OH (2 M), and no inert gas, such as nitrogen, was bubbled through the reaction mixture. This sample is referred to as HT-NO_3.

The MgAl-CH_3COO^- LDH was prepared by the co-precipitation method. Two aqueous solutions (200 mL), the first one containing 0.15 mol of ($Mg(CH_3CO_2)_2{\cdot}4H_2O$) and 0.05 mol of ($Al(CH_3CO_2)_2$. OH) for a composition Mg/Al = 3 and the second one containing 0.4 mol of NaOH and 0.05 mol of ($NaCH_3CO_2$), were slowly mixed at 50 °C under vigorous stirring, maintaining the pH close to 10. The mixture is refluxed at 65 °C at the end of the addition for 18 h. The precipitate was washed several times, and the products were dried at 80 °C. This sample is referred to as HT-CH_3COO. They were made active by employing a tube furnace to calcinate the catalysts, HT-CO_3, HT-NO_3 and HT-CH_3COO, to 450 °C in the air. The temperature was maintained at 450 °C for 8 h while increasing by 5 °C/min. The catalyst-produced mixed oxides are used to condense the furfural and acetone.

2.3. Reaction conditions and analysis

In a stirred auto-clave agitation reactor set to the reaction temperature, furfural was aldol condensed with acetone. For each experiment, the reactor is filled with 29 g of acetone (A) and 4.8 g of furfural (F) (molar ratio A/F = 10). Acetone was added more than furfural to produce FA with remarkable selectivity (Xu et al., 2011) and then given 1 g of freshly calcined cHT-X hydrotalcite. Using decane as an internal standard, GC is used to track the dissolution of furfural and the development of condensation products (FA and F2A). The injector and detector temperatures were set at 250 °C. The temperature of the column was programmed by heating it at 50 °C for 3 min, then ramping up at a rate of 20 °C/min to 150 °C, leaving it at this temperature for 3 min, then

ramping up at a rate of 2 °C/min. The chromatographic analysis was performed using a (Shimadzu-2010) chromatograph equipped with a DB1 capillary column 0.25 mm in diameter and 25 m in length and a flame ionization detector. The reaction products have been identified by comparing them to commercial items based on their retention times.

The following formulas were used to calculate the conversion rates of furfural, selectivity, and yield to FA and F2A at a given moment.

$$\text{conversion}\,(\%) = \frac{[F]_0 - [F]_t}{[F]_0} 100 selectivity_{FA}(\%) = \frac{[FA]_t}{[F]_0 - [F]_t} 100$$

$$yield_{product(i)}(\%) = \frac{[product(i)]_t}{[F]_0}.100\, selectivity_{F2A}(\%) = \frac{2[FA]_t}{[F]_0 - [F]_t} 100$$

Where $[F]_0$, $[F]_t$, $[FA]_t$, and $[F2A]_t$ represents the starting concentration of furfural, the concentration at the time of furfural that has not yet been consumed, and the concentrations of the products FA and F2A.

2.4. Catalysts characterization

Monochromatized Cu-K radiation (λ = 1.5406 Å, 40 kV, and 20 mA) was used in a PW 1800 Philips automated goniometer (Bragg-Brentano) to record hydrotalcite samples' powder X-ray diffraction patterns. The data were gathered using angular increments of 0.04° to 2S per increment over the 2θ angular diffraction range of 5° to 70°. The hydrotalcite samples Fourier transformed infrared (FT-IR) spectra were captured using the KBr pellet technique and a Shimadzu (IR AFFINITY-1S) instrument, with a resolution of 4 cm^{-1} for each sample. The KBr pellets were made by combining 98 wt—% KBr with extensively dried hydrotalcite with around 2 wt% of KBr.

They used a Shimadzu thermogravimetric and differential thermal analyzer (TG-DTA) analysis (TA-60). Samples weighing a few milligrams were heated at 10 °C/min until 600 °C. Using a scanning electron microscope, the TESCAN Vega3-EDAX apparatus with an accelerating voltage of 20 kV examined the morphology of the Hydrotalcites powder. Our materials' elemental makeup was identified using energy-dispersive X-ray spectroscopy (EDS). Specific surface areas and pore sizes for the catalysts calcined (cHT-X) were determined by the BET (Brunauer-Emmet- Teller) and BJH (Barrett-Joyner-Hallenda) method, respectively, from the N_2 isotherms carried at −196 °C using a Micromeritics ASAP-2010 system. The catalysts were outgassed under a vacuum at 200 °C prior to analysis.

An acid-base titration method was performed to quantitatively determine the total basicity of the calcined solids (cHT-X). Before the measurement, all catalysts were carefully degassed at a temperature of 110 °C. In this method, 150 mg of solids were dissolved in 2 mL (0.1 mg. L^{-1}) of a freshly prepared phenolphthalein indicator solution in toluene and stirred at room temperature for 45 min. The resulting solution was titrated with aqueous benzoic acid (0.01 M).

3. Results and discussions

3.1. Catalysts characterization

3.1.1. XRD

According to Fig. 1, the XRD patterns of all the synthesized samples have strong, symmetric basal reflections at low values of 2θ, indicative of the LDHs structure (Miyata, 1980). The broad and asymmetric XRD peaks at larger values of 2θ indicate that the hydrotalcite phase is severely disordered. The samples of HT-NO_3 and HT-CH_3COO are very distinct. The reflections are an R3m rhombohedral symmetric hexagonal lattice (Arhzaf et al., 2020b). The basal distance between the layers was calculated using the (0 0 3) reflection, using the formula $c = 3d_{003}$. The (1 1 0) reflection was used to calculate the unit cell dimension a where $a = 2d_{110}$. The crystal size was measured from the X-ray peak using the Sherrer equation (Holzwarth & Gibson, 2011; Houssaini et al., 2021).

$$D = \frac{k.\lambda}{\beta}.\frac{1}{\cos(\theta)}$$

Where (k) is a constant related to the crystallite shape, normally taken to be equal to 0.9, with (λ) the X-ray wavelength, (β) is the width of the diffraction peak at half maximum, and (θ) is the value of the theta angle relative to a line (0 0 3). The results show that the size of the crystals varied depending on the sort of intercalated anion, as seen in Table 1. For HT-CO_3 and HT-NO_3, the diffraction patterns consist of more extensive reflections at higher 2θ values and crisp, symmetric, and strong basal reflections at low 2θ values, corresponding to consecutive orders of the interlayer spacing. The basal reflections for HT-CH_3COO are more diffuse and less intense, which suggests less crystallinity and a disorder of the layered structure. As a result, the anion's type determines the hydrotalcite's crystallinity and layering sequence. XRD patterns of cHT-X show that the hydrotalcite layered structure disappears when heated to 450 °C and then cooled again. The only reflections in the XRD pattern pertain to the MgO phase, indicating the development of Mg-Al mixed oxide with the MgO periclase-type structure, where the results are shown in (Table 1).

The lattice parameter (a) is the same for all the solids since they are

Table 1
Lattice parameters and size crystallite of the hydrotalcite samples.

Sample	d (0 0 3) (Å)	c (Å)	d (1 1 0) (Å)	a (Å)	D (0 0 3) (Å)
HT-CO_3	7.81	23.43	1.531	3.06	90
HT-NO_3	8.67	26.02	1.526	3.05	52
HT-CH_3COO	12.10	36.30	1.529	3.06	64

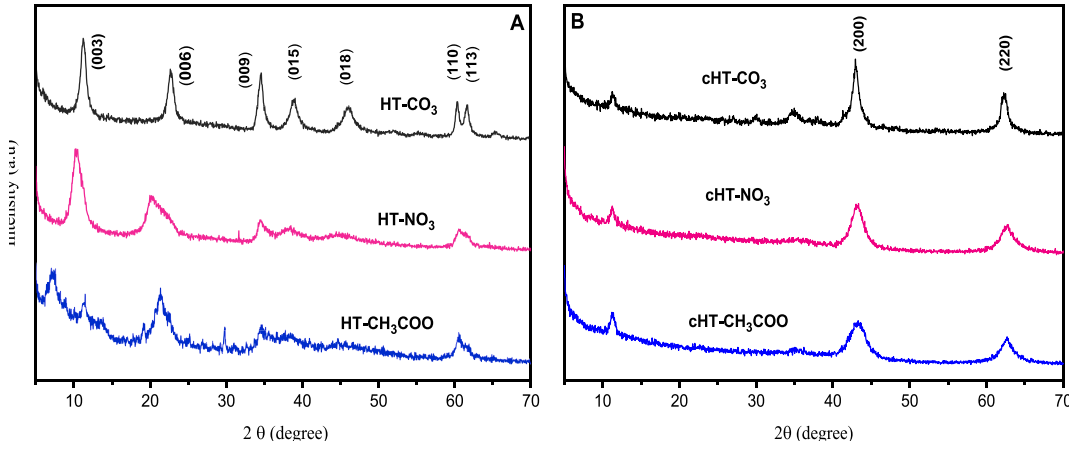

Fig. 1. X-ray diffraction patterns of the fresh hydrotalcite (A: HT-X) and calcined hydrotalcites (B: cHT-X).

the same types of metal atoms, Mg and Al. The significant difference in the basal spacing is due to anions intercalating in the different solids, where the charge and size of anions lead to the smallest parameter value (c). Monocharged anions, such as NO_3^- and CH_3COO^-, increase parameter (c), compared to the anions CO_3^{2-} that are doubly charged and cause a strong electrostatic attraction. The intercalation of acetate anions, with an average spacing of 12.1 Å ($2\theta = 7.2°$), corresponds to the (0 0 3) reflection in acetate intercalated LDHs, like the report of El Malki et al (El Malki et al., 1992). The higher order basal reflections, (0 0 6) and (0 0 9), are observed at $2\theta = 11.5°$ (7.6 Å) and $2\theta = 21.3°$ (4.2 Å), respectively. The turbostratic disorder in the middle region ($30° < 2\theta < 50°$) is due to the disordered insertion of water molecules in the interlayer galleries of HT-CH_3COO.

3.1.2. FT-IR

Infrared spectroscopy has been widely used to characterize hydrotalcite and related materials (Abelló et al., 2005; Xu et al., 1998). The samples IR spectra are displayed in (Fig. 2). In every instance, intense and broad absorptions caused by hydroxyls and water molecules physically adsorbed and in the interlayer (OH stretching modes) at 3600–3400 cm^{-1} and (OH bending mode) at 1640–1600 cm^{-1} were seen (Bish and Brindley, 1978; Miyata, 1975; Sharma et al., 2007). The asymmetric stretching of the carbonate and nitrate anions was attributed to the bands at 1370 and 1382 cm^{-1} for the samples. The CO_3^{2-} and NO_3^- out-of-plane deformation was characterized by the bands at 836 and 854 cm^{-1}. In the HT-CH_3COO sample, the bands at 1561 cm^{-1} and 1412 cm^{-1} represent the symmetric and antisymmetric stretching vibrations of the COO^- groups. The bands seen at lower wavenumbers in the spectrum (400 $cm^{-1} < \nu < 1000$ cm^{-1}) are thought to be lattice vibration modes associated with M−O and M−OH vibrations (Titulaer et al., 1994).

3.1.3. TGA-DTA

Fig. 3 depicts the thermal breakdown of samples in the air using TG-DTA analysis over the temperature range of (25–600) °C. The breakdown profiles have a total weight loss in the range of (35–46) wt%, which is in good accord with those reported in the literature for hydrotalcite-like compounds (Morato et al., 2001; Prinetto et al., 2000). The thermograms of the three LDHs materials, HT-CO_3, HT-NO_3, and HT-CH_3COO show two zones of weight loss corresponding to endothermic events in the DTA analysis (Reichle et al., 1986). Lossing physically adsorbed and interlayer water molecules account for the first peak at the region below 207 °C, with a weight loss of (11–18) wt% (Arhzaf et al., 2021). Whereas the second peak between (297–497) °C is caused by the dehydroxylation of the brucite-like sheets and the breakdown of the compensating anions in the interlayer (Cavani et al., 1991). However, for HT-NO_3 in this temperature domain, the pic is vast due to the stability of nitrate ions. In addition to the two weight loss peaks previously mentioned, HT-CH_3COO also showed a third powerful and extremely narrow exothermic peak at 435 °C, which was caused by the breakdown of acetate anions (Fig. 3). We can infer that the interlayer anion's type offsets the DTA peaks but only slightly affects the overall weight loss.

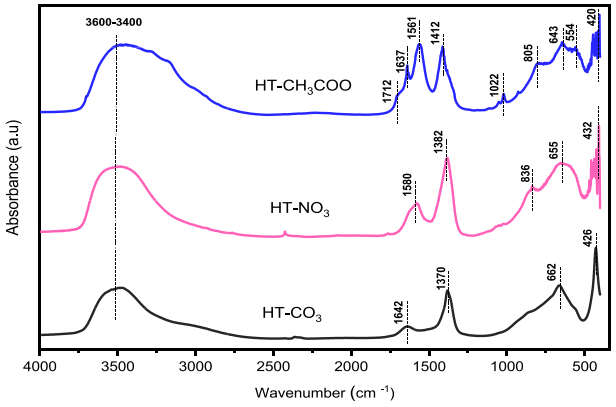

Fig. 2. FT-IR spectra of the HT-X Hydrotalcites.

3.1.4. SEM-EDS

The scanning electron microscopy images obtained for the three synthesized materials are shown in Fig. 4. The morphologies significantly differ according to the intercalated anion, and the inter-lamellar anion's nature strongly modifies the platelets' morphology, size and aggregation state. The composition of the platelets was probed by energy-dispersive X-ray spectroscopy (EDS). The results of the EDS analyses are presented in Table 2 and indicate the existence of Mg and Al with their atomic composition close to 3 for HT-CO_3 (Mg/Al = 2.95) and HT-NO_3 (Mg/Al = 3.14) while for the HT-CH_3COO phase, the atomic composition is different from the expected one (Mg/Al = 1.98). This could be from the total precipitation in the acetate anion case.

3.1.5. BET

The experimental measurement of the specific surface area is based on nitrogen adsorption according to the principle of the Brunauer, Emmet, and Teller methods (Yukselen and Kaya, 2006). It is easily deduced by knowing the surface area occupied by a nitrogen molecule (N_2), and the volume adsorbed on the catalyst's monolayer. The nitrogen adsorption–desorption isotherms at −196 °C performed on the calcined solids catalysts are shown in Fig. 5. It is shown that the isotherms obtained for three solids correspond to type IV (mesoporous solids) according to the IUPAC classification. The hysteresis loop is of type H3, indicating the formation of the catalysts in platelets, typical of hydrotalcite materials (Zhang et al., 2019). This isotherm is found in materials which have aggregates that are non-rigid and of platelet particles forming pores of slit shape. The textural properties of the calcined solids are summarized in Table 3. The average pore size of the solids is in the range of (10–18 nm), confirming that all samples are mesoporous materials. The BET surface area of the calcined hydrotalcites varied in the range from 69 to 179 $m^2.g^{-1}$. Among the studied samples, the calcined HT-NO_3 hydrotalcite is characterized by the lowest surface area (69 $m^2.g^{-1}$). It is likely that the stability of the nitrate anions after calcination close to 450 °C, as shown in the figures of the TG-DTA analysis, causes the blocking of the pores and thus decreases the porous volume (0.12 $cm^3.g^{-1}$). Contrary to cHT-NO_3 the total pore volume of the other samples is relatively high, ranging from 0.27 $cm^3.g^{-1}$ for cHT-CH_3COO to 0.74 $cm^3.g^{-1}$ for cHT-CO_3. The high porosity of cHT-CO_3 compared to cHT-CH_3COO could be explained by the presence of pores with diameters in the 14–18 nm range.

3.1.6. Total basicity

Titration is a common analytical technique used to determine a solid's concentration or the amount of base. The total basicity of the calcined solids was determined by titration with benzoic acid (pKa = 4.2) (Sahu et al., 2013), using phenolphthalein as an indicator. We then calculated the basicity of different solids from the amount of benzoic acid consumed during the titration. Prior to calcination, the three prepared hydrotalcites (HT-X) had lower base strength because they could not change the color of the phenolphthalein ($8.0 < pK_{BH+} < 9.6$). In contrast, with heat treatment, the calcined Mg-Al hydrotalcites had a higher base strength, which increases in the order cHT-NO_3 < cHT-CH_3COO < cHT-CO_3 according to the Hammett basicity measurements shown in Table 4, which show that the strength of the most robust base sites of these materials depends on their composition.

It is clear from the literature that the basic surface properties of these materials depend on the nature of the M^{2+} and M^{3+} cations, their M^{2+}/M^{3+} molar ratio or the nature of their compensating anions. When considering the effect of the nature of the compensating anions on the materials on its basicity, two situations must be distinguished. With

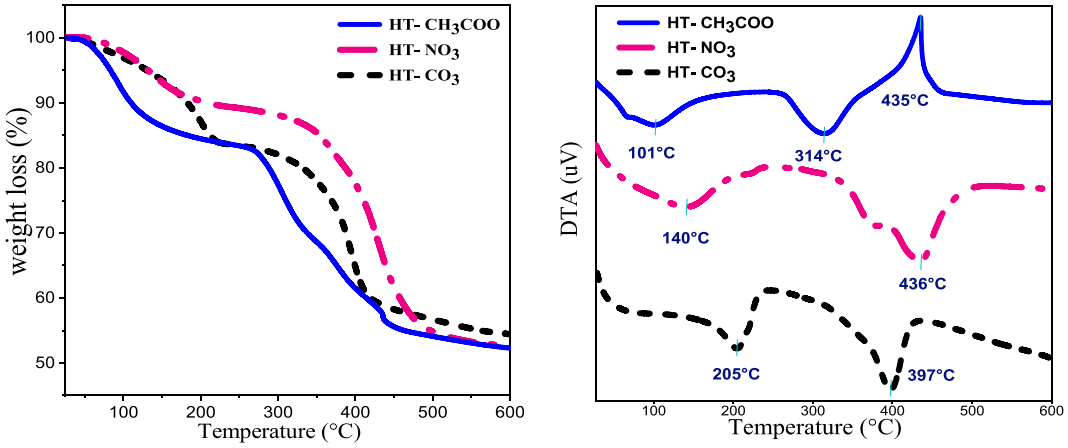

Fig. 3. TGA–DTA profiles in the (25–600) °C range of HT-X hydrotalcite.

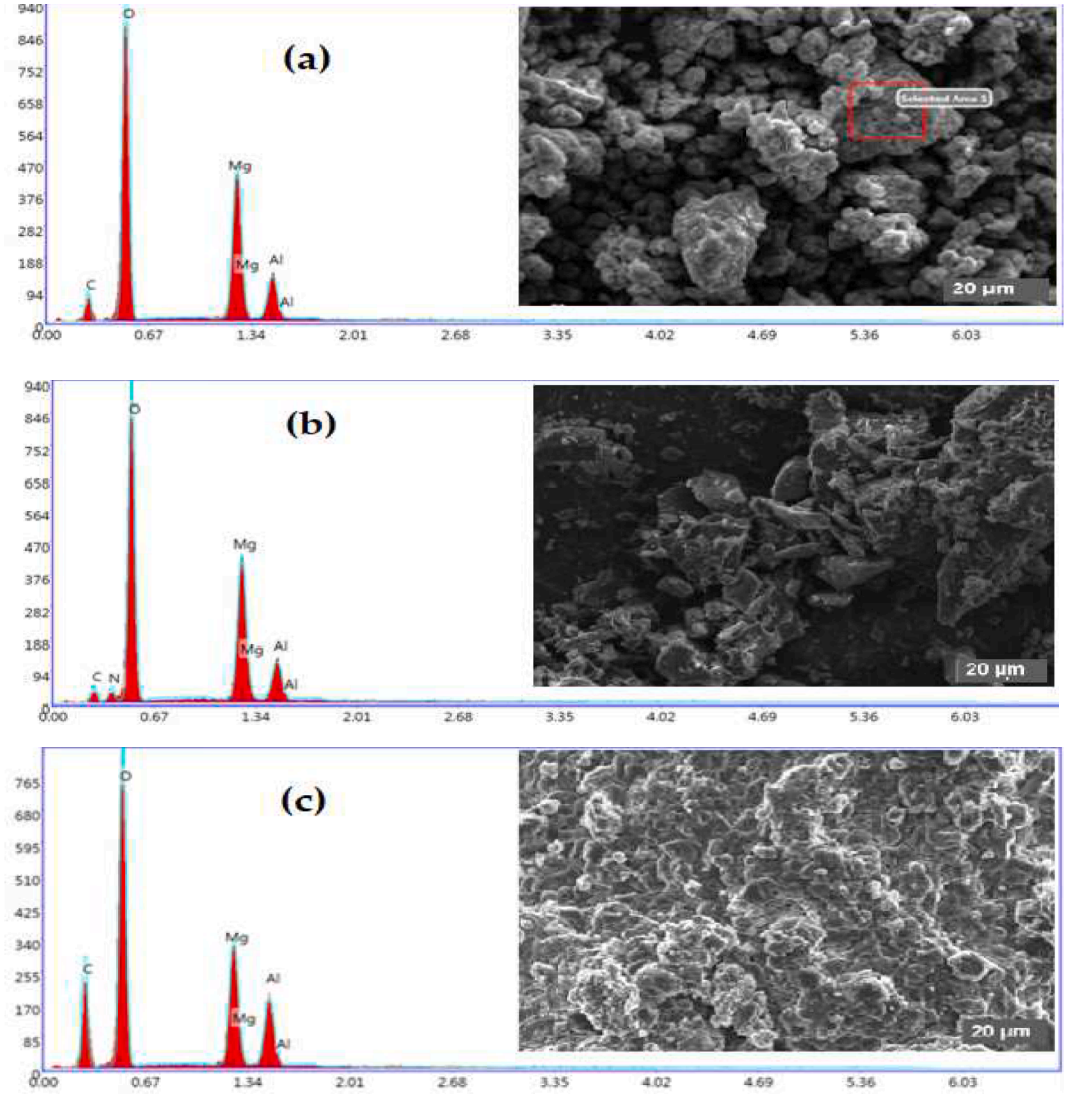

Fig. 4. SEM images at 20 µm and EDS analysis of the hydrotalcite: (a) HT-CO_3, (b) HT-NO_3 and (c) HT-CH_3COO.

fresh or rehydrated hydrothalcite, basicity is primarily controlled by the nature of the intercalated anion and the amount of water remaining (Abelló et al., 2005; D. Tichit et al., 1998). In calcined hydrotalcite, the surface concentration of the base centers varies with the type of anion inserted in the hydrotalcite (Kustrowski et al., 2004). For the calcined hydrothalcite HT-CO_3 and HT-CH_3COO, the active base sites are associated with hydroxide and various acid-base pairs of Lewis, like Mg^{2+}-–O_2^- or Al^{3+}–O_2^- and a Lewis base associated with O_2^- anions (Climent

Table 2
EDS elemental data analysis of hydrotalcite samples.

Samples	Atomic percent in (%)				
	C	N	O	Mg	Al
HT-CO_3	15.91	-	58.45	19.15	6.49
HT-CH_3COO	33.28	-	49.94	11.15	5.63
HT-NO_3	8.59	6.14	60.13	19.07	6.07

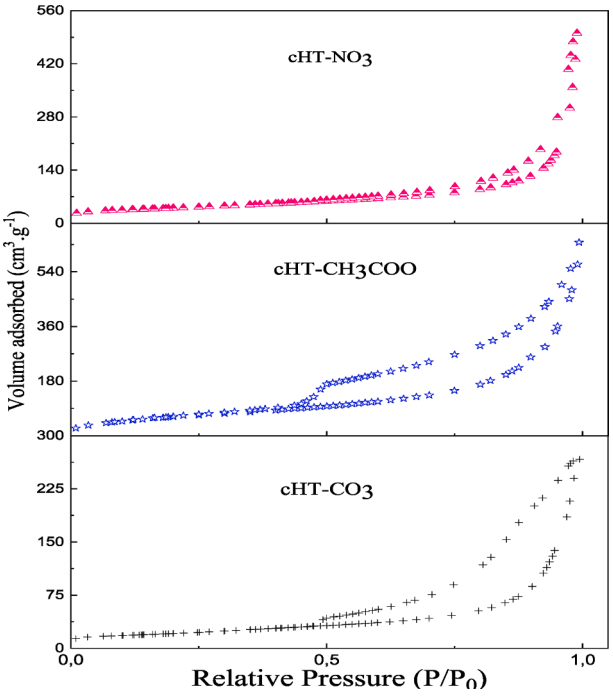

Fig. 5. Nitrogen adsorption/desorption isotherms for calcined MgAl-Hydrotalcites. Fig. 5 Reaction scheme of the aldol condensation between Furfural and Acetone.

Table 3
Surface area and porosity of the calcined solids are determined by N_2 adsorption.

SSample	Surface BET ($m^2.g^{-1}$)	Pore diameter (nm)	Pore volume ($cm^3.g^{-1}$)
cHT-CO_3	179	14 – 18	0.74
cHT-NO_3	69	10 – 12	0.12
cHT-CH_3COO	121	12 – 16	0.27

Table 4
Total basicity of the calcined solids.

Sample	Total Basicity (mmol. g^{-1})	Total Basicity ($mmol.m^{-2}$)	Base strength
cHT-CO_3	3.20	0.018	$11.1 < pK_{BH+} < 12.7$
cHT-NO_3	0.42	0.006	
cHT-CH_3COO	2.87	0.024	$8.0 < pK_{BH+} < 9.6$ $10.1 < pK_{BH+} < 11.1$

et al., 2004). In addition, the weak base sites in hydrotalcites come from OH– groups, while strong base sites in calcined hydrotalcites are associated with OH– groups and O_2^- centers related to metal atoms. The results of the total basicity measured on the various catalysts are presented in Table 3, which show that the number of total basicity in ($mmol.m^{-2}$) of the calcined Mg-Al hydrotalcites (cHT-X) increases in the order cHT-NO_3 < cHT-CO_3 < cHT-CH_3COO. It shows that the type of interlayer anion in precursor hydrotalcites significantly affects the calcined Mg-Al hydrotalcites' surface basicity.

3.2. Catalytic activity in the aldol condensation reaction of furfural with acetone

The modifications of the properties of the catalyst resulting from the insertion of the different X^{n-} anions followed by calcination were more characterized by their performance in aldol condensation of furfural with acetone. The aldol condensation between acetone and furfural using the hydrotalcite-type solid catalysts is according to the following reaction (Fig. 5) (Hora et al., 2014). As we know, the first step in this condensation reaction is the extraction of a proton from the α-carbon atom of acetone (A) through a basic catalytic site, forming a carbanion which consecutively attacks the carbonyl group of the adjacently adsorbed furfural molecule. From this reaction, an intermediate β-hydroxyl ketone (alcohol) formed and dehydrated quickly to yield a first condensation product, 4-(2-furyl)-3-buten-2-one (FA). The initial abstraction of the α obtains the F2A (1,4-pentadien-3-one, 1,5-di-2-furanyl) -proton from FA, forming a carbanion which attacks successively the carbonyl group from another absorbed furfural molecule (Medina et al., 2007). In a parallel route, the probable auto-condensation of acetone on the calcined hydrotalcites was negligible, corresponding to an acetone conversion not exceeding 1.5 %. The intermediate carbanion formed from acetone could attack a second acetone molecule leading to diacetone alcohol and mesityl oxide.

Catalytic activity for calcined hydrotalcites is illustrated in Table 5 at 60 and 90 °C, respectively. In preliminary tests, the catalytic performance of the three prepared hydrotalcites (HT-X) was assessed in aldol condensation of furfural and acetone at 60 °C and acetone/furfural ratio of 10. Regardless of origin of X anions, furfural conversion does not exceed 2 % in all cases, thus proving the absence of strong basicity in the as prepared hydrotalcites. It was confirmed by the low basic strength of these materials compared to the calcined hydrotalcites and the high surface area and porosity of the calcined hydrotalcites were essential to obtain high catalytic activity. The lower conversion of furfural through cHT-NO_3 is due to its low basicity and low porosity, however, for cHT-CO_3 and cHT-CH_3COO the conversion is the same and exceeds 74 % at 60 °C, and 98 % at 90 °C. The density of the base sites in cHT-CH_3COO (0.024 $mmol.m^{-2}$) greater than that in cHT-CO_3 (0.018 $mmol.m^{-2}$) was probably the factor responsible for increasing the selectivity of F2A for the catalyst in acetate (32 % at 90 °C) compared to that of carbonate (18 % at 90 °C).

Furfural conversion and catalyst selectivity was significantly influenced by temperature and reaction time. The conversion reaction at lower temperatures, less than acetone boiling point, caused poorer starting materials conversions to furfural and selectivity desirable condensation selectivity products FA and F2A. The critical reaction step is forming alcohol intermediate in the early stages of the reaction, which is then dehydrated to give the first desired condensation product, FA. This is condensed with another furfural molecule and dehydrated to produce F2A. According to Lukas Hora et al. (Hora et al., 2014), a low temperature does not favor dehydration of the alcohol intermediate in the initial state of the reaction, which decreases the selectivity of the reaction towards FA and F2A at the expense of the alcohol intermediate, whereas high temperature (60–90) °C favors the synthesis of condensation products with better selectivity over FA (Table 5).

The calcined solids derived from carbonates and acetates exhibit a large specific surface area, which contributes to their excellent activity in the condensation reaction between furfural and acetone. However, there is a difference in selectivity towards the formation of FA and F2A. When the calcined solid based on carbonates is used at a temperature of 90 °C, the reaction achieves a conversion rate of 99 % after two hours, with a selectivity of 76 % towards FA and 18 % towards F2A. On the other hand, the calcined solid based on acetates shows a selectivity

Table 5
Conversion and selectivity of calcined LDHs, in the aldol condensation between acetone and furfural at 60 and 90 °C after 2 h of reaction.

Sample	T (°C)	Conversion % of Furfural	Selectivity % of FA	Selectivity % of F2A	Yield % of FA	Yield % of F2A
cHT-CO_3	60	76	50	17	38	12.9
cHT-NO_3	90	99	76	18	73.7	17.5
cHT-CH_3COO	60	08	38	06	03	0.5
	90	12	41	09	4.9	1.1
	60	74	42	23	31	17
	90	98	65	32	60	30

conversion of 65 % towards FA and 32 % towards F2A. This variation in selectivity can be attributed to differences in the density, strength, and nature of the basic sites present in the calcined hydrotalcites, as well as disparities in the porosity and specific surface area of these materials.

4. Conclusions

The MgAl-X (HT-X) phases were synthesized using the co-precipitation method at a constant pH, with a fixed molar ratio of Mg/Al = 3, and different compensating anions (X: CO_3^{2-}, NO_3^-, and CH_3COO^-). Various physicochemical techniques were employed to characterize these materials. X-ray diffraction (XRD) analysis revealed that the diffractograms of the synthesized lamellar phases closely resembled those of layered double hydroxides. Electron microscopic observations confirmed the distinct platelet morphology of these phases, which varied depending on the intercalated anion. FT-IR analysis helped identify molecular vibrations corresponding to the interlamellar anions, hydroxyl groups, and network vibrations related to the octahedral layers. Following calcination, the resulting materials (cHT-X) exhibited mesoporous characteristics, with textural properties influenced by the type of interlayer anion in the initial hydrotalcite. The composition of the parent solid (HT-X) also affected the density and strength of the basic surface sites. In comparison to the aldol condensation of furfural with acetone, the mixed oxide cHT-NO_3 derived from HT-NO_3 displayed low catalytic activity. Conversely, the mixed oxides cHT-CO_3 and cHT-CH_3COO derived from HT-CO_3 and HT-CH_3COO, respectively, exhibited excellent conversion to furfural (≥98 %). Selectivity differences were observed towards FA and F2A, with the cHT-CO_3 catalyst demonstrating higher selectivity towards FA (76 % at T = 90 °C) compared to cHT-CH_3COO (65 % at T = 90 °C). Conversely, the cHT-CH_3COO catalyst displayed higher selectivity towards F2A (32 %) than the cHT-CO_3 catalyst (18 %) at the same temperature (90 °C). Furthermore, both catalysts showed increased conversion and selectivity with higher temperatures.

Funding

This research was funded by the Ministry of Higher Education and the National Center for Scientific and Technical Research (CNRST), Morocco.

Declaration of competing interest

The authors declare that they have no known competing financial interests or personal relationships that could have appeared to influence the work reported in this paper.

References

Abd El-Monaem, E.M., Elshishini, H.M., Bakr, S.S., El-Aqapa, H.G., Hosny, M., Andaluri, G., El-Subruiti, G.M., Omer, A.M., Eltaweil, A.S., 2023. A comprehensive review on LDH-based catalysts to activate persulfates for the degradation of organic pollutants. npj Clean Water 6. https://doi.org/10.1038/s41545-023-00245-x.

Abdelrahman, A.A., Bendary, S.H., Mahmoud, S.A., 2023. Synthesis and electrochemical properties of Ni–Al LDH@RGO hierarchical nanocomposite as a potential counter electrode in dye sensitized solar cells. Diam. Relat. Mater. 134, 109738 https://doi.org/10.1016/j.diamond.2023.109738.

Abelló, S., Medina, F., Tichit, D., Pérez-Ramírez, J., Groen, J.C., Sueiras, J.E., Salagre, P., Cesteros, Y., 2005. Aldol condensations over reconstructed Mg-Al hydrotalcites: Structure-activity relationships related to the rehydration method. Chem. - A Eur. J. 11, 728–739. https://doi.org/10.1002/chem.200400409.

Arhzaf, S., Naciri Bennani, M., Abouarnadasse, S., Ziyat, H., Qabaqous, O., 2020b. Effect of Mg/Al molar ratio on the basicity of Mg-Al mixed oxide derived from Mg-Al hydrotalcite. Mediterr. J. Chem. 10, 625. https://doi.org/10.13171/mjc10602007021464sa.

Arhzaf, S., Naciri Bennani, M., Abouarnadasse, S., Ziyat, H., Qabaqous, O., 2020a. Effect of Mg/Al molar ratio on the basicity of Mg-Al mixed oxide derived from Mg-Al hydrotalcite. Mediterr. J. Chem. 10, 625. https://doi.org/10.13171/mjc10602007021464sa.

Arhzaf, S., Bennani, M.N., Abouarnadasse, S., Houssaini, J., Ziyat, H., Qabaqous, O., 2021. Solvent-free aldol condensation of furfural and acetone on calcined Mg-Al hydrotalcites. Moroccan J. Chem. 9, 614–627. https://doi.org/10.48317/IMIST.PRSM/morjchem-v9i3.23587.

Bendary, S.H., Abdelrahman, A.A., 2022. Flexible and novel counter electrode from graphene/Zn Al layered double hydroxide nanocomposite in dye sensitized solar cells. J. Electroanal. Chem. 922, 116736 https://doi.org/10.1016/j.jelechem.2022.116736.

Bish, D.L., Brindley, G.W., 1978. Deweylites, mixtures of poorly crystalline hydrous serpentine and talc-like minerals. Mineral. Mag. 42, 75–79. https://doi.org/10.1180/minmag.1978.042.321.09.

Cavani, F., Trifirò, F., Vaccari, A., 1991. Hydrotalcite-type anionic clays: Preparation, properties and applications. Catal. Today 11, 173–301. https://doi.org/10.1016/0920-5861(91)80068-K.

Climent, M.J., Corma, A., Iborra, S., Epping, K., Velty, A., 2004. Increasing the basicity and catalytic activity of hydrotalcites by different synthesis procedures. J. Catal. 225, 316–326. https://doi.org/10.1016/j.jcat.2004.04.027.

Debecker, D.P., Gaigneaux, E.M., Busca, G., 2009. Exploring, tuning, and exploiting the basicity of hydrotalcites for applications in heterogeneous catalysis. Chem. - A Eur. J. 15, 3920–3935. https://doi.org/10.1002/chem.200900060.

El Malki, K., Guenane, M., Forano, C., De Roy, A., Besse, J.P., 1992. Inorganic and organic anionic pillars intercalated in lamellar double hydroxides. Mater. Sci. Forum 91–93, 171–176. https://doi.org/10.4028/www.scientific.net/msf.91-93.171.

Eltaweil, A.S., Bakr, S.S., Abd El-Monaem, E.M., El-Subruiti, G.M., 2023. Magnetic hierarchical flower-like Fe3O4@ZIF-67/CuNiMn-LDH catalyst with enhanced redox cycle for Fenton-like degradation of Congo red: optimization and mechanism. Environ. Sci. Pollut. Res. 30, 75332–75348. https://doi.org/10.1007/s11356-023-27430-2.

Holzwarth, U., Gibson, N., 2011. The Scherrer equation versus the "Debye-Scherrer equation". Nat. Nanotechnol. 6, 534. https://doi.org/10.1038/nnano.2011.145.

Hora, L., Kelbichová, V., Kikhtyanin, O., Bortnovskiy, O., Kubička, D., 2014. Aldol condensation of furfural and acetone over MgAl layered double hydroxides and mixed oxides. Catal. Today 223, 138–147. https://doi.org/10.1016/j.cattod.2013.09.022.

Hora, L., Kikhtyanin, O., Čapek, L., Bortnovskiy, O., Kubička, D., 2015. Comparative study of physico-chemical properties of laboratory and industrially prepared layered double hydroxides and their behavior in aldol condensation of furfural and acetone. Catal. Today 241, 221–230. https://doi.org/10.1016/j.cattod.2014.03.010.

Houssaini, J., Naciri Bennani, M., Ziyat, H., Arhzaf, S., Qabaqous, O., Amhoud, A., 2021. Study of the catalytic activity of the compounds hydrotalcite type treated by microwave in the self-condensation of acetone. Int. J. Anal. Chem. 2021 https://doi.org/10.1155/2021/1551586.

Houssaini, J., Naciri Bennani, M., Arhzaf, S., Mounir, C., Alaqarbeh, M., Ahlafi, H., Amhoud, A., 2023a. Solvent-free synthesis of jasminaldehyde over chitosan–layered double hydroxide catalyst assisted by microwave irradiation. Arab. J. Chem. 16, 105326 https://doi.org/10.1016/j.arabjc.2023.105326.

Houssaini, J., Naciri Bennani, M., Arhzaf, S., Ziyat, H., Alaqarbeh, M., 2023b. Effect of microwave method on jasminaldehyde synthesis using solvent-free over Mg–Al–NO3 hydrotalcite catalyst. Arab. J. Chem. 16, 105316 https://doi.org/10.1016/j.arabjc.2023.105316.

Kikhtyanin, O., Hora, L., Kubička, D., 2015. Unprecedented selectivities in aldol condensation over Mg-Al hydrotalcite in a fixed bed reactor setup. Catal. Commun. 58, 89–92. https://doi.org/10.1016/j.catcom.2014.09.002.

Kikhtyanin, O., Tišler, Z., Velvarská, R., Kubička, D., 2017. Reconstructed Mg-Al hydrotalcites prepared by using different rehydration and drying time: Physico-chemical properties and catalytic performance in aldol condensation. Appl. Catal. A Gen. 536, 85–96. https://doi.org/10.1016/j.apcata.2017.02.020.

Kuśtrowski, P., Chmielarz, L., Bozek, E., Sawalha, M., Roessner, F., 2004. Acidity and basicity of hydrotalcite derived mixed Mg-Al oxides studied by test reaction of MBOH conversion and temperature programmed desorption of NH3 and CO2. Mater. Res. Bull. 39, 263–281. https://doi.org/10.1016/j.materresbull.2003.09.032.

Medina, F., Tichit, D., Pe, J., 2007. Aldol condensation of campholenic aldehyde and MEK over activated hydrotalcites 70, 577–584. https://doi.org/10.1016/j.apcatb.2006.01.021.

Miyata, S., 1975. The syntheses of hydrotalcite-like compounds and their structures and physico-chemical properties-i: The systems Mg2+-Al3+-No3-, Mg2+-Al3+-Cl-, Mg2+-Al3+-ClO4-, Ni2+-Al3+-Cl- and Zn2+-Al3+-Cl-. Clays Clay Miner. 23, 369–375. https://doi.org/10.1346/ccmn.1975.0230508.

Miyata, S., 1980. Physico-chemical properties of synthetic hydrotalcites in relation to composition. Clays Clay Miner. 28, 50–56. https://doi.org/10.1346/ccmn.1980.0280107.

Morato, A., Alonso, C., Medina, F., Cesteros, Y., Salagre, P., Sueiras, J.E., Tichit, D., Coq, B., 2001. Palladium hydrotalcites as precursors for the catalytic hydroconversion of CC12F2 (CFC-12) and CHC1F2 (HCFC-22). Appl. Catal. B Environ. 32, 167–179. https://doi.org/10.1016/S0926-3373(01)00140-0.

Parejas, A., Cosano, D., Hidalgo-Carrillo, J., Ruiz, J.R., Marinas, A., Jiménez-Sanchidrián, C., Urbano, F.J., 2019. Aldol condensation of furfural with acetone over Mg/Al mixed oxides. Influence of water and synthesis method. Catalysts 9, 1–12. https://doi.org/10.3390/catal9020203.

Prinetto, F., Ghiotti, G., Graffin, P., Tichit, D., 2000. Synthesis and characterization of sol-gel Mg/Al and Ni/Al layered double hydroxides and comparison with co-precipitated samples. Micropor. Mesopor. Mater. 39, 229–247. https://doi.org/10.1016/S1387-1811(00)00197-9.

Reichle, W.T., Kang, S.Y., Everhardt, D.S., 1986. The nature of the thermal decomposition of a catalytically active anionic clay mineral. J. Catal. 101, 352–359. https://doi.org/10.1016/0021-9517(86)90262-9.

Sahu, P.K., Sahu, P.K., Gupta, S.K., Agarwal, D.D., 2013. Role of calcinations and basicity of hydrotalcite as catalyst for environmental benign novel synthesis of 4H-pyrimido [2,1-b][1,3]benzothiazole derivatives of curcumin. Cat. Sci. Technol. 3, 1520–1530. https://doi.org/10.1039/c3cy20807a.

Serhan, M., Sprowls, M., Jackemeyer, D., Long, M., Perez, I.D., Maret, W., Tao, N., Forzani, E., 2019. Total iron measurement in human serum with a smartphone. AIChE Annu. Meet. Conf. Proc. 2019-Novem. https://doi.org/10.1039/x0xx00000x.

Sharma, S.K., Kushwaha, P.K., Srivastava, V.K., Bhatt, S.D., Jasra, R.V., 2007. Effect of hydrothermal conditions on structural and textural properties of synthetic hydrotalcites of varying Mg/Al ratio. Ind. Eng. Chem. Res. 46, 4856–4865. https://doi.org/10.1021/ie061438w.

Sudheesh, N., Sharma, S.K., Khokhar, M.D., Shukla, R.S., 2011. Kinetic investigations on the modified chitosan catalyzed solvent-free synthesis of jasminaldehyde. J. Mol. Catal. A Chem. 339, 86–91. https://doi.org/10.1016/j.molcata.2011.02.016.

Tichit, D., Naciri Bennani, M., Figueras, F., Tessier, R., Kervennal, J., 1998. Aldol condensation of acetone over layered double hydroxides of the meixnerite type. Appl. Clay Sci. 13, 401–415. https://doi.org/10.1016/S0169-1317(98)00035-0.

Tichit, D., Bennani, M.N., Figueras, F., Ruiz, J.R., 1998. Decomposition processes and characterization of the surface basicity of Cl- and CO32- hydrotalcites. Langmuir 14, 2086–2091. https://doi.org/10.1021/la970543v.

Tichit, D., Lutic, D., Coq, B., Durand, R., Teissier, R., 2003. The aldol condensation of acetaldehyde and heptanal on hydrotalcite-type catalysts. J. Catal. 219, 167–175. https://doi.org/10.1016/S0021-9517(03)00192-1.

Tichit, D., 1998. Aldol condensation of acetone over layered double hydroxides of the meixnerite type 401–415.

Titulaer, M.K., Jansen, J.B.H., Geus, J.W., 1994. The quantity of reduced nickel in synthetic takovite: Effects of preparation conditions and calcination temperature. Clays Clay Miner. 42, 249–258. https://doi.org/10.1346/CCMN.1994.0420303.

Trave, A., Selloni, A., Goursot, A., Tichit, D., Weber, J., 2002. First principles study of the structure and chemistry of Mg-based hydrotalcite-like anionic clays. J. Phys. Chem. B 106, 12291–12296. https://doi.org/10.1021/jp026339k.

West, R.M., Liu, Z.Y., Peter, M., Gärtner, C.A., Dumesic, J.A., 2008. Carbon-carbon bond formation for biomass-derived furfurals and ketones by aldol condensation in a biphasic system. J. Mol. Catal. A Chem. 296, 18–27. https://doi.org/10.1016/j.molcata.2008.09.001.

Xing, R., Subrahmanyam, A.V., Olcay, H., Qi, W., van Walsum, G.P., Pendse, H., Huber, G.W., 2010. Production of jet and diesel fuel range alkanes from waste hemicellulose-derived aqueous solutions. Green Chem. 12, 1933–1946. https://doi.org/10.1039/c0gc00263a.

Xu, M., Iglesia, E., Apestegu, C.R., Cosimo, D.I., Al, E.T., 1998. Structure and Surface and Catalytic Properties of Mg-Al Basic Oxides 510, 499–510.

Xu, W., Liu, X., Ren, J., Liu, H., Ma, Y., Wang, Y., Lu, G., 2011. Synthesis of nanosized mesoporous Co-Al spinel and its application as solid base catalyst. Micropor. Mesopor. Mater. 142, 251–257. https://doi.org/10.1016/j.micromeso.2010.12.008.

Yukselen, Y., Kaya, A., 2006. Comparison of methods for determining specific surface area of soils. J. Geotech. Geoenviron. Eng. 132, 931–936. https://doi.org/10.1061/(asce)1090-0241(2006)132:7(931).

Zhang, C.Y., Shao, W.L., Zhou, W.X., Liu, Y., Han, Y.Y., Zheng, Y., Liu, Y.J., 2019. Biodiesel production by esterification reaction on k+ modified mgal-hydrotalcites catalysts. Catalysts 9. https://doi.org/10.3390/catal9090742.